SCIENTIFIC REPORTS

OPEN

SUBJECT AREAS:
BATTERIES
ELECTRONIC MATERIALS
STRUCTURAL PROPERTIES
ELECTRONIC PROPERTIES AND DEVICES

Received
8 April 2013

Accepted
17 July 2013

Published
1 August 2013

Correspondence and requests for materials should be addressed to W.H. (wei-huang@njupt.edu.cn) or T.Y. (yuting@ntu.edu.sg)

A Novel Graphene-Polysulfide Anode Material for High-Performance Lithium-Ion Batteries

Wei Ai[1,2], Linghai Xie[2], Zhuzhu Du[2], Zhiyuan Zeng[3], Juqing Liu[3,4], Hua Zhang[3], Yunhui Huang[5], Wei Huang[2,4] & Ting Yu[1,6]

[1]Division of Physics and Applied Physics, School of Physical and Mathematical Sciences, Nanyang Technological University, 637371, Singapore, [2]Key Laboratory for Organic Electronics & Information Displays (KLOEID) and Institute of Advanced Materials (IAM), Nanjing University of Posts and Telecommunications, 9 Wenyuan Road, Nanjing 210046, P. R. China, [3]School of Materials Science and Engineering, Nanyang Technological University, 639798, Singapore, [4]Jiangsu-Singapore Joint Research Center for Organic/Bio-Electronics & Information Displays and Institute of Advanced Materials, Nanjing University of Technology, Nanjing 211816, P. R. China, [5]State Key Laboratory of Material Processing and Die & Mould Technology, School of Materials Science and Engineering, Huazhong University of Science and Technology, Wuhan, Hubei 430074, P. R. China, [6]Department of Physics, Faculty of Science, National University of Singapore, 117542, Singapore.

We report a simple and efficient approach for fabrication of novel graphene-polysulfide (GPS) anode materials, which consists of conducting graphene network and homogeneously distributed polysulfide in between and chemically bonded with graphene sheets. Such unique architecture not only possesses fast electron transport channels, shortens the Li-ion diffusion length but also provides very efficient Li-ion reservoirs. As a consequence, the GPS materials exhibit an ultrahigh reversible capacity, excellent rate capability and superior long-term cycling performance in terms of 1600, 550, 380 mAh g^{-1} after 500, 1300, 1900 cycles with a rate of 1, 5 and 10 A g^{-1} respectively. This novel and simple strategy is believed to work broadly for other carbon-based materials. Additionally, the competitive cost and low environment impact may promise such materials and technique a promising future for the development of high-performance energy storage devices for diverse applications.

With the increasing global demand for energy in recent years, development of energy conversion and storage technologies faces many opportunities and challenging simultaneously[1]. Rechargeable lithium-ion batteries (LIBs), one of the most promising candidates for energy storage devices, which have been widely used in portable electronics now request further development to possess super high energy and power density, and excellent cycling stability[2]. Conventional LIBs configuration consists of lithium transition metal oxides or phosphates as the positive electrode (cathode) and graphite-type materials as the negative electrode (anode). Charge storage capability is inherently limited to about 300 mAh g^{-1}, due to the low theoretical specific capacity of the cathode (150–200 mAh g^{-1}) and the anode (372 mAh g^{-1}) materials[3,4]. Thus, significant research efforts have been focused on searching advanced carbon-based anode materials with enhanced Li ion storage capacity for next-generation LIBs. Up-to-date, various carbon-based materials, such as carbon nanotube[5], carbon fiber[6], porous carbon[7] and their hybrids[8] have been well investigated as a possible anode material for LIBs. Graphene and its derivatives have also been considered as a potential electrode material for LIBs[9–11], primarily due to its extraordinary electrical conductivity, large specific surface area and stable chemical property. However, the facile synthesis of graphene anode materials for high performance LIBs, especially suitable for mass-scalable preparation remains challenging.

Organosulfur compounds, such as organodithiols, organodisulfides and organosulfur polymers have been widely explored for the promising electrode materials in recent years, owing to their high theoretical capacity, low cost and environmental benign[12]. In particular, organosulfur polymers have attracted tremendous attention own to the truth that such polymer contains large content of S-S bonds[13], which could effectively release and store energy through the reversible S-S bond cleavage and recombination during the discharge/charge processes[14]. Unfortunately, these compounds usually suffer from the rapid capacity fading just like their elemental sulfur electrode counterpart due to the similar mechanism of electrode dissolution[15]. Graphene oxide (GO), results from the chemical exfoliation of graphite, can be regarded as a large, disordered, but two-dimensional polymer

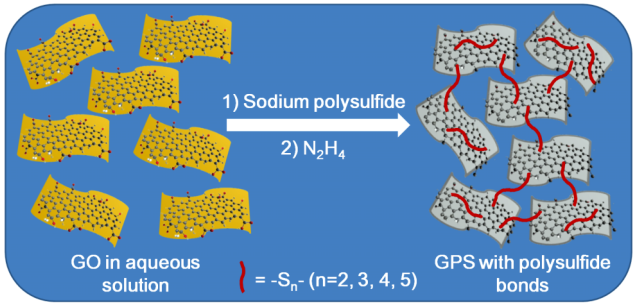

Figure 1 | Schematic illustration of the fabrication process to integrate polysulfide bonds to the basal plane of graphene. The GPS materials were prepared via the nucleophilic addition reactions between carbonyl and epoxy groups on GO with the polysulfide ions, and subsequent reduction by hydrazine.

functionalized with a range of reactive oxygen-containing groups. Therefore, it would be natural to chemically introduce polysulfide bonds onto GO sheet. Consequently, the synergistic effect of combining the high capacity feature of organosulfur polymers with the good electrical conductivity and Li ion storage performance of graphene is established in the GPS materials, which simultaneously solve the issue of sulfide dissolution due to the C-S bonds.

Herein, we report a novel and very efficient method for synthesis of graphene-polysulfide (GPS) through the treatment of GO with sodium polysulfide, and subsequent reduction by hydrazine. The formation of polysulfide bonds attached to the basal plane of graphene involves the nucleophilic addition reactions between carbonyl and epoxy groups on GO with the polysulfide ions. The resultant GPS materials are demonstrated to be an anode material for high performance LIBs in terms of ultrahigh reversible capacity, excellent rate capability and superior long-term cycling performance. The GPS battery is able to deliver a capacity of 1600 mAh g^{-1} after 600 cycles at a current density of 1 A g^{-1} or 380 mAh g^{-1} after 1900 cycles at 10 A g^{-1}. In general, the significantly improved electrochemical performance of the LIBs can be ascribed to the unique architecture of GPS such as graphene sheets with the abundant polysulfide bonds can ensure the ultrahigh storage of Li-ions because of the great abilities of storing Li-ions of both two types of reservoirs (graphene and polysulfide bonds) and the recovery of sp^2 carbon network structure for fast electron transfer between the active materials and current collector. Most importantly, this simple and efficient strategy can be broadly applied to other carbon-based materials, such as carbon nanotubes, carbon fibers, carbon spheres and porous carbon, which may open up the possibility for the development of novel functionalized carbon-based anode materials for high performance LIBs.

Results

The method used to synthesize GPS materials is illustrated in Figure 1. In a typical procedure, sodium polysulfide solution containing polysulfide anions of controlled chain lengths was dropwised into the GO suspension (pH = 7 ~ 8) in the presence of sodium dodecyl sulfate (SDS) under N_2 atmosphere with continuous stirring. The suspension was heated to complete the reaction, and then reduced by hydrazine to further improve the conductivity of the GPS materials. The as-obtained graphene-polysulfide, abbreviated as G2S, G3S, G4S and G5S corresponding to the length of the polysulfide chains, respectively, were filtrated and washed with deionized water for several times, then dried in vacuum.

Discussion

The chemical composition of the GPS materials were studied by Fourier transformed infrared spectroscopy (FT-IR), X-ray photoelectron spectroscopy (XPS) and Raman spectroscopy. In the FT-IR spectrum of GO (Fig. 2a), three characteristic adsorption bands at 1733, 1229 and 1053 cm^{-1} present, corresponding to the C=O, C-OH and C-O stretching vibrations, respectively[16]. These peaks disappear in the spectra of the GPS materials. Instead, two new adsorption bands at 1167 and 710 cm^{-1} representing the C-S and S-S stretching vibrations are clearly seen. This affirms the polysulfide bonds have been successfully introduced to the graphene sheets[17,18]. Compared to graphene oxide-pentasulfide (GO5S), the band at 1543 cm^{-1} is attributed to the N-H bending vibration, due to the aromatic nitrogen doping during the reduction process with hydrazine[19]. The C-N bond in the C 1s XPS spectra of G5S and the decreased peak intensity of the oxygen-containing groups in the spectra of the GPS materials further confirm the reduction of GPS materials (Fig. S1)[20]. Besides C 1s and O 1s peaks for all the samples, S 2p peak at 162.1 eV is clearly seen in the spectra of the GPS materials (Fig. S2), demonstrating the sulfur has been effectively introduced to graphene sheets. To further confirm the bonding configurations of S atoms, the GPS materials were investigated by analyzing the high-resolution S 2p XPS spectra (Fig. 2b and Fig. S3). The S 2p peak of the GPS materials could be fitted as three peaks at binding energies of about 163.4, 164.7 and 168.2 eV, respectively. The two lower energy peaks correspond to the C-S bond[21] and S-S bond[22], respectively,

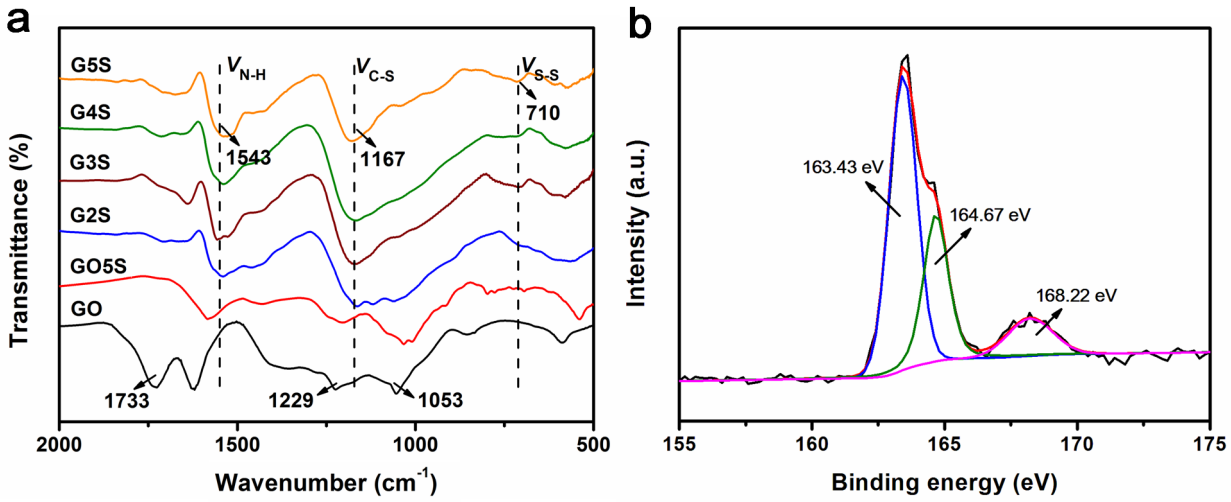

Figure 2 | Structural analysis of GO and GPS. (a) FT-IR spectra of GO, GO5S, G2S, G3S, G4S and G5S. (b) High-resolution S 2p spectrum of G5S, indicating the polysulfide bonds have been successfully introduced to the graphene sheets.

confirming the presence of chemical bonding between polysulfide and graphene sheet. The weak peak at about 168.2 eV could be attributed to the unwashed sulfate ion in GPS materials[23].

The Raman spectra of both GO and GPS materials show two remarkable peaks around 1340 and 1589 cm^{-1}, assigned to the defects or disorders (D band) and the E_{2g} mode (G band) (Fig. S4)[9,16], respectively. In the Raman spectra of the GPS materials, the frequency of the D and G band are very similar to that observed in GO. It is noted that the I_D/I_G ratios of the GPS materials are larger than that of GO, which could be due to the introducing structural disorder and doping by the formation of polysulfide bonds on graphene sheets[9]. The GPS materials were further characterized by powder X-ray diffraction (XRD) measurements (Fig. S5). The pristine graphite shows sharp crystalline peaks at $2\theta = 26.5^\circ$ and 54.7° corresponding to (002) and (004) planes, respectively. For GPS materials, the strongest diffraction peak ((002) plane) appears at about $2\theta = 23^\circ$, corresponding to a d-spacing of 0.386 nm, which is much lower than that of GO precursor (0.711 nm) while slightly higher than the pristine graphite (0.336 nm). These results suggest the introduction of polysulfide bonds can partially prevent the restacking of graphene sheets. Notably, longer polysulfide bonds bonded on graphene sheets could result in a larger d-spacing, as reflected by a downwards shift of the diffraction peak, and thus facilitate the rapid diffusion of Li-ions.

The morphologies of GO and the as-prepared GPS materials were investigated by field-emission scanning electron microscopy (FESEM) and transmission electron microscopy (TEM). Due to the hydrophilicity and ionizability of the oxygen-containing groups, graphite oxide can be readily exfoliated in water to yield stable dispersions of single-layer GO (Fig. S6). The size distribution of GO is in the range of hundreds nanometers to several micrometers, with a thickness of about 1.1 nm (Fig. S6 and Fig. S7). While the GPS materials exhibit a graphite-like structure due to the restacking of the functionalized graphene sheets (Fig. 3a and Fig. S7). In addition, the existence of S in GPS has been confirmed by energy dispersive X-ray spectrometry (EDS) analysis (inset of Fig. 3a, Fig. S7 and Fig. S8). The weight fraction of S in GPS materials can be determined from thermogravimetric analysis (TGA). The TGA curves are provided in Fig. S9. The total S atomic weight ratio is calculated to be ~ 52% for G5S, ~ 21% for G4S, ~ 19% for G3S and ~ 16% for G2S, respectively. TEM image reveals that GO consists of thin flake-like shapes, resembling transparent and rippled silk waves. Elemental mapping of carbon and oxygen indicates the homogeneous distribution of oxygen on graphene sheets (Fig. S10). However, the GPS materials exhibit randomly aggregated, thin and crumpled sheets interconnected with each other as shown in Fig. 3b and Fig. S11. This structure may favorably improve the electrochemical performance of the GPS materials, owing to the electrically conducting network of graphene sheets[24]. Meanwhile, the carbon and sulfur elemental mapping clearly demonstrates that sulfur is homogeneously distributed in the GPS materials (Fig. 3c, 3d and Fig. S11).

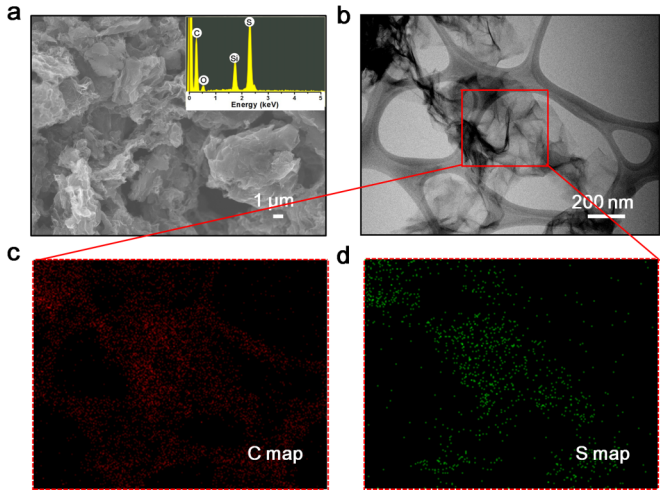

Figure 3 | The morphological analysis of G5S by FESEM and TEM. (a) FESEM image of G5S. Inset: EDS spectra of GPS showing the presence of sulfur. (b) TEM image of G5S with corresponding elemental mapping images of (c) carbon and (d) sulfur in the selected area, indicating the homogeneous distribution of sulfur in G5S.

The lithium storage properties of the GPS materials were further investigated by using the standard GPS/Li half-cell configuration. It can be seen that the cyclic voltammogram (CV) curves of the GPS electrodes are not the same as the carbon-based materials[6,9], but similar as the reported organosulfur compounds[25], another evidence of the formation of polysulfide bonds on the graphene sheets. As shown in Fig. 4a and Fig. S13, there are two pairs of redox peaks at about 1.92/2.00 and 2.43/1.54 V, respectively, indicating the redox reaction on GPS electrodes processed in two steps as schematically discussed in the support information (Fig. S12). The cathodic peak at about 2.00 V is due to the cleavage of the long S-S chains to general lithium polysulfide, while another cathodic peak at about 1.54 V is attributed to the conversion of lithium polysulfide to Li_2S. The two anodic peaks observed at about 1.92 and 2.43 V should be assigned to the recombination of S-S bond[18]. Figure 4b and Figure S13 show the charge/discharge curves of the GPS electrodes at a current of 250 mA g^{-1} between 0.005 and 3.0 V (vs. Li/Li^+). During the first cycle, the voltage drops rapidly and then forms a plateau at 1.75–1.25 V, which is due to the lithium insertion reaction with polysulfide bonds[14]. Thereafter, a plateau is also observed at 1.00–0.70 V due to the formation of solid electrolyte interface (SEI) film on the surface of the GPS materials and other side reactions[6,9]. It can be seen that the first discharge and charge capacities of G5S are as high as 2435 and 1488 mAh g^{-1}, respectively, corresponding to a coulombic efficiency of 61.1%. The irreversible capacity could be associated with the formation of the SEI in the first cycle and the trapping of Li-ions at some locations of electrode materials. However, a stable and reversible capacity with coulombic efficiency over 99% is observed after the first few cycles as discussed in detail below. Notably, after the first discharge, the flat plateau at 1.75–1.25 V is substituted by a sloping curve due to the heterogeneous reaction mechanism of Li insertion and extraction[26,27], which matches well with the shape of the CV curves. The presence of polysulfide bonds on graphene sheets could still be observed after hundreds of cycles (Fig. S14).

The plots of the charge/discharge capacity and coulombic efficiency versus cycle number for the GPS electrodes are evaluated between 0.005 and 3.0 V (vs. Li/Li^+) at a current of 250 mA g^{-1} (Fig. 4c and Fig. S13). It is interesting to observe that the capacity of the GPS electrodes decreases in the first 50 (roughly) cycles, and then gradually increases as the cycle number increases, which could be attributed to the activating process of the GPS electrode[6,9]. Two aspects can be taken into account for this increase in capacity[28]: (I) the first discharge induces the sudden volume expansion of the active layer due to a large amount of Li-ions insertion into the GPS materials, which may block the further Li-ions transfer from electrode to electrolyte. Therefore, part of the Li_2S is possibly left in the GPS materials after the first charge, consequently the capacity decreases in the succeeding cycles. This is also responsible for the low coulombic efficiency in the first cycle. (II) After a number of cycles of Li-ions insertion/extraction, the GPS materials become more expanded and porous as demonstrated by FESEM (Fig. S15), which could effectively promote the electrolyte to access the inner part of the active materials. Thus, the trapped Li_2S can re-exposure to the electrolyte and release Li-ions. Meanwhile, the contacting area of the GPS materials with the electrolyte could also be enhanced, resulting in the increase of both the capacity and coulombic efficiency to be over 99%. It is also noted that the capacity is much larger for the longer polysulfide chain, that is capacity of G5S > G4S > G3S > G2S, due to the

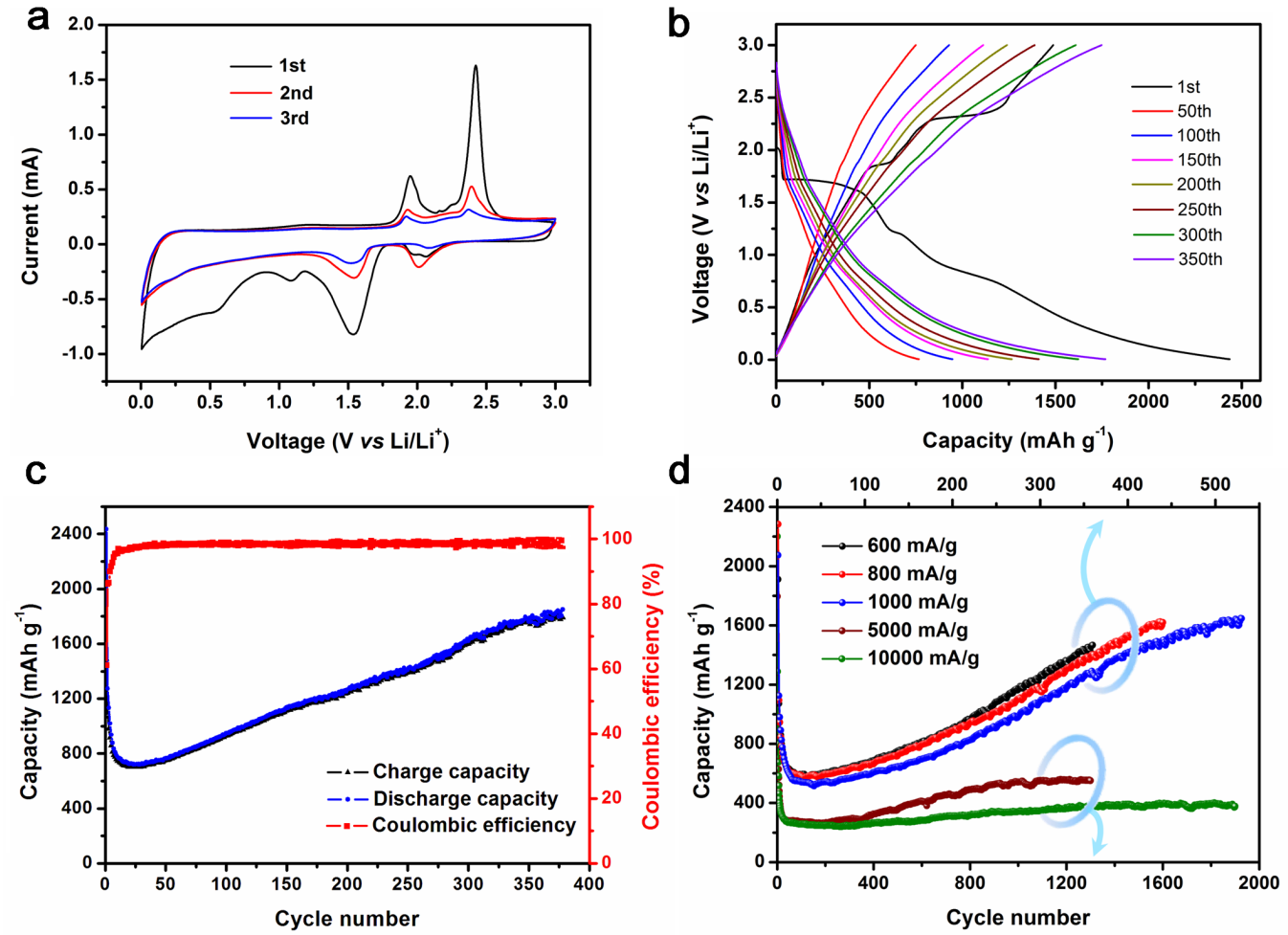

Figure 4 | Electrochemical lithium storage performance of G5S electrode. (a) CV curves of G5S electrode at a scan rate of 0.5 mV s^{-1} over a voltage range of 0.005 to 3.0 V (vs. Li/Li^+). (b) The discharge-charge curves of G5S electrode at a current of 250 mA g^{-1}. (c) Cycling performance of the G5S electrode tested at a current density of 250 mA g^{-1}. (d) Cycling performance of the G5S electrode at various current densities.

significantly increased S-S bonds content in the GPS materials (Fig. S9). On the other hand, the enhanced conductivity of graphene with longer polysulfide chain, demonstrated by the electrochemical impedance spectroscopy (EIS) (Fig. S16) could be also responsible for such enhancement of capacity. More importantly, the capacity of G5S can be retained at 1850 mAh g^{-1} after 380 cycles with coulombic efficiency over 99% per cycle after the first few cycles, which is much higher, actually 5 times of that of the commercially used graphite (372 mAh g^{-1}) and the other reported carbon-based anode materials[6,9].

The rate capability is an important parameter for many applications of batteries. Figure 4d shows that the G5S material exhibits high lithium storage and excellent cycling stability even at very high rates. The capacities can sustain as high as 1467, 1620, 1600, 550 and 380 mAh g^{-1} at charging/discharging rates of 600, 800, 1000, 5000 and 10000 mA g^{-1} after 360, 440, 500, 1300, 1900 cycles. The ultrahigh capacity, long-term cycling performance and excellent coulombic efficiency of the GPS materials could be attributed to the unique architecture of GPS. First, graphene sheets can be the excellent conductive agent by providing channels for electrons transportation, shortening the diffusion length of Li-ions and fastening Li-ions diffusion from electrolyte to electrode due to its large interfacial area. Second, graphene sheets with the abundant polysulfide bonds can ensure the ultrahigh storage of Li-ions because of the great abilities of storing Li-ions of both two types of reservoirs (graphene and polysulfide bonds). Third, the dissolution of polysulfides can be effectively prevented due to the covalent bond between the polysulfides and graphene. Based on our findings, it can be concluded that high performance carbon-based anode materials for LIBs can be achieved by integrating of polysulfide bonds on the carbon-based materials.

In summary, we have successfully developed a general method for the synthesis of novel GPS anode materials for high performance LIBs, based on the nucleophilic addition reactions between carbonyl and epoxy groups on GO with the polysulfide ions. The unique structural features of the GPS materials such as the homogenous distribution of sulfur on graphene sheets and electrically conducting network of graphene sheets, lead to the superior electrochemical performance in terms of ultrahigh reversible capacity, excellent rate capability and superior long-term cycling performance. We believe that our strategy could be broadly applied to other carbon-based materials, which may open up a new pathway for the realization of various functionalized carbon-based anode materials for high performance LIBs.

Methods

Materials. Graphite powder (< 20 μm), sulfuric acid (H_2SO_4), potassium permanganate ($KMnO_4$), hydrogen peroxide (H_2O_2), sodium sulfide nonahydrate ($Na_2S{\cdot}9H_2O$), sulfur (S), SDS, hydrazine monohydrate ($NH_2NH_2{\cdot}H_2O$) were purchased from Sigma-Aldrich Pte Ltd and used without further purification.

Preparation of GO suspension. Graphite oxide was synthesized from graphite (Aldrich; < 20 μm) by a modified Hummers' method following the procedures

reported earlier[29]. GO solution (2 mg mL^{-1}) was prepared by ultrasonic exfoliation of graphite oxide (800 mg) into deionized water (400 mL) for 50 min. The pH value of the solution was adjusted to 7 ~ 8 by the addition of a few drops of KOH solution, followed by 10 min centrifugation at 1000 rpm to remove the unexfoliated particles. After that SDS (1 g) was added into the solution and sonicated for another 5 min to obtain GO suspension.

Preparation of sodium polysulfide solutions. $Na_2S{\cdot}9H_2O$ (3.85 g) was added into 70 mL deionized water, and then S powder was added under continuous stirring and sonication until a transparent solution was achieved. To control the length of the polysulfide chain, different content of S powder was added, such as 0.512 g S for disulfide, 1.024 g S for trisulfide, 1.536 g S for tetrasulfide and 2.048 g S for pentasulfide. The color of the solution changed from bright yellow to yellow-brown with increasing the length of the polysulfide chain through the following reaction:

$$Na_2S + (x-1)\,S = Na_2S_x\ (x = 2,3,4,5)$$

Preparation of graphene-polysulfide materials. The as-prepared sodium polysulfide solutions were dropwised into the GO suspension under N_2 atmosphere, and then refluxed at 80°C for 24 h. The product was collected by filtration and washed with deionized water for several times, then redispersed into deionized water (400 mL) by sonication for 5 min. Afterwards, hydrazine monohydrate (7 mL) was added and refluxed at 80°C for 24 h. The obtained graphene-polysulfide, abbreviated as G2S, G3S, G4S and G5S according to the length of the polysulfide chains, respectively, were filtrated and washed with deionized water for several times, then dried in vacuum at 120°C for 12 h.

Characterization. FT-IR was recorded on a NEXUS 670 spectrometer by using pressed KBr pellets. XPS analysis was performed on an ESCALAB MK II X-ray photoelectron spectrometer. FESEM analysis was performed on a JEOL JSM-6700F electron microscope with an EDX spectrometer. TEM measurements were conducted on a JEOL JEM-2010 transmission electron microscope with an accelerating voltage of 200 kV. XRD analysis was performed using a D8 Advanced diffractometer with Cu Kα line (λ = 1.54056 Å). Raman spectra were collected using a WITEC CRM200 Raman system with 532 nm excitation laser. TGA was recorded by a Shimadzu DTG-60H under a heating rate of 10°C/min and a nitrogen flow rate of 50 cm^3 min^{-1}.

Electrochemical measurements. The working electrodes were prepared by mixing 80 wt% of the graphene-polysulfide, 10 wt% of acetylene black (Super-P) and 10 wt% of polyvinylidene difluoride dissolved in N-methyl-2-pyrrolidone to form a slurry. The obtained slurry was coated onto a copper foil current collector, which was then dried in vacuum at 90°C for 12 h to remove the solvent. Electrochemical measurements were performed using 2032 coin-type cells with lithium metal as the counter electrode. The electrolyte was 1 mol L^{-1} $LiPF_6$ in a 50 : 50 (w/w) mixture of ethylene carbonate and dimethyl carbonate. The coin cells were assembled inside an argon-filled glove box with both moisture and oxygen contents below 0.1 ppm. The galvanostatic charge/discharge tests were performed using a NEWARE battery testing system in the voltage range of 0.005–3.0 V (vs. Li/Li^+). The capacity values were calculated based on the weight of GPS materials loaded on the copper foil. CV measurements were performed on CHI 760D electrochemical workstation using a voltage range of 0.005 to 3.0 V (vs. Li/Li^+) at a scan rate of 0.5 mV s^{-1}. EIS was conducted on CHI 760D electrochemical workstation.

1. Goodenough, J. B. & Kim, Y. Challenges for Rechargeable Li Batteries. *Chem. Mater.* **22**, 587–603 (2009).
2. Tarascon, J. M. & Armand, M. Issues and challenges facing rechargeable lithium batteries. *Nature* **414**, 359–367 (2001).
3. Ji, X., Lee, K. T. & Nazar, L. F. A highly ordered nanostructured carbon-sulphur cathode for lithium-sulphur batteries. *Nat. Mater.* **8**, 500–506 (2009).
4. Wang, Z., Zhou, L. & Lou, X. W. Metal Oxide Hollow Nanostructures for Lithium-ion Batteries. *Adv. Mater.* **24**, 1903–1911 (2012).
5. Zhou, G. *et al.* A nanosized Fe_2O_3 decorated single-walled carbon nanotube membrane as a high-performance flexible anode for lithium ion batteries. *J. Mater. Chem.* **22**, 17942–17946 (2012).
6. Qie, L. *et al.* Nitrogen-Doped Porous Carbon Nanofiber Webs as Anodes for Lithium Ion Batteries with a Superhigh Capacity and Rate Capability. *Adv. Mater.* **24**, 2047–2050 (2012).
7. Lee, K. T., Lytle, J. C., Ergang, N. S., Oh, S. M. & Stein, A. Synthesis and Rate Performance of Monolithic Macroporous Carbon Electrodes for Lithium-Ion Secondary Batteries. *Adv. Funct. Mater.* **15**, 547–556 (2005).
8. Hassoun, J. & Scrosati, B. A High-Performance Polymer Tin Sulfur Lithium Ion Battery. *Angew. Chem. Int. Ed.* **49**, 2371–2374 (2010).
9. Yan, Y., Yin, Y. X., Xin, S., Guo, Y. G. & Wan, L. J. Ionothermal synthesis of sulfur-doped porous carbons hybridized with graphene as superior anode materials for lithium-ion batteries. *Chem. Commun.* **48**, 10663–10665 (2012).
10. Ji, H. *et al.* Ultrathin Graphite Foam: A Three-Dimensional Conductive Network for Battery Electrodes. *Nano Lett.* **12**, 2446–2451 (2012).
11. Yang, S. *et al.* Porous Iron Oxide Ribbons Grown on Graphene for High Performance Lithium Storage. *Sci. Rep.* **2**, 427 (2012).
12. Liang, Y., Tao, Z. & Chen, J. Organic Electrode Materials for Rechargeable Lithium Batteries. *Adv. Energy Mater.* **2**, 742–769 (2012).
13. Fanous, J., Wegner, M., Grimminger, J., Andresen, A. & Buchmeiser, M. R. Structure-Related Electrochemistry of Sulfur-Poly(acrylonitrile) Composite Cathode Materials for Rechargeable Lithium Batteries. *Chem. Mater.* **23**, 5024–5028 (2011).
14. Krishnan, P., Advani, S. G. & Prasad, A. K. Synthesis and evaluation of polythiocyanogen (SCN)x as a rechargeable lithium-ion battery electrode material. *J. Power Sources* **196**, 7755–7759 (2011).
15. Wang, H. *et al.* Graphene-Wrapped Sulfur Particles as a Rechargeable Lithium-Sulfur Battery Cathode Material with High Capacity and Cycling Stability. *Nano Lett.* **11**, 2644–2647 (2011).
16. Marcano, D. C. *et al.* Improved Synthesis of Graphene Oxide. *ACS Nano.* **4**, 4806–4814 (2010).
17. Brownridge, S. *et al.* The Highest Bond Order Between Heavier Main-Group Elements in an Isolated Compound? Energetics and Vibrational Spectroscopy of $S_2I_4(MF_6)_2$ (M = As, Sb). *Inorg. Chem.* **44**, 1660–1671 (2005).
18. Zhang, S. C., Zhang, L., Wang, W. K. & Xue, W. J. A Novel cathode material based on polyaniline used for lithium/sulfur secondary battery. *Synth. Met.* **160**, 2041–2044 (2010).
19. Park, S. *et al.* Chemical structures of hydrazine-treated graphene oxide and generation of aromatic nitrogen doping. *Nat. Commun.* **3**, 638 (2012).
20. Stankovich, S. *et al.* Synthesis of graphene-based nanosheets via chemical reduction of exfoliated graphite oxide. *Carbon* **45**, 1558–1565 (2007).
21. Boyer, C. *et al.* The stabilization and bio-functionalization of iron oxide nanoparticles using heterotelechelic polymers. *J. Mater. Chem.* **19**, 111–123 (2009).
22. Kohli, P., Taylor, K. K., Harris, J. J. & Blanchard, G. J. Assembly of Covalently-Coupled Disulfide Multilayers on Gold. *J. Am. Chem. Soc.* **120**, 11962–11968 (1998).
23. Shao, X., Tian, J., Xue, Q. & Ma, C. Fabrication of MoO_3 nanoparticles on an MoS_2 template with $(C_4H_9Li)MoS_2$ exfoliation. *J. Mater. Chem.* **13**, 631–633 (2003).
24. Ai, W. *et al.* Benzoxazole and benzimidazole heterocycle-grafted graphene for high-performance supercapacitor electrodes. *J. Mater. Chem.* **22**, 23439–23446 (2012).
25. Zhang, J. *et al.* Poly(ethene-1,1,2,2-tetrathiol): Novel cathode material with high specific capacity for rechargeable lithium batteries. *J. Power Sources* **186**, 496–499 (2009).
26. Poizot, P., Laruelle, S., Grugeon, S., Dupont, L. & Tarascon, J. M. Nano-sized transition-metal oxides as negative-electrode materials for lithium-ion batteries. *Nature* **407**, 496–499 (2000).
27. Poizot, P., Laruelle, S., Grugeon, S. & Tarascon, J. M. Rationalization of the low-potential reactivity of 3d-metal-based inorganic compounds toward Li. *J. Electrochem. Soc.* **149**, A1212–A1217 (2002).
28. Ji, H. X. *et al.* Self-Wound Composite Nanomembranes as Electrode Materials for Lithium Ion Batteries. *Adv. Mater.* **22**, 4591–4595 (2010).
29. Shang, J. *et al.* The Origin of Fluorescence from Graphene Oxide. *Sci. Rep.* **2**, 792 (2012).

Acknowledgments

This work is supported by the Singapore National Research Foundation under NRF RF Award No. NRFRF2010-07. LHX and WH thank the support of the "973" project (No. 2009CB930600, 2012CB933301), NNSFC (Grants No. 21144004, 61136003, 51173081, 20974046, 50428303), the Program for New Century Excellent Talents in University (NCET-11-0992), the Ministry of Education of China (No. IRT1148), the NSF of Jiangsu Province (Grants No. SBK201122680, 11KJB510017, BK2008053, 11KJB510017, BZ2010043 and No.BK2009025) and NUPT (No. NY210030 and NY211022). WA thanks the help of Dr. Shi Chen and Mr. Ng Chin Fan for the XPS measurement of the G5S after 400 cycles.

Author contributions

W.A. and T.Y. initialled the project, conceived and designed the experiments; W.A. and T.Y. performed the battery tests; W.A., Z.Z.D. and L.H.X. conducted FTIR and XPS measurements. W.A., Z.Y.Z., J.Q.L. and H.Z. did the TEM. W.A. and T.Y. collected and analysed the data and co-wrote the paper with W.H. and Y.H.H. All authors discussed the results and commented on the manuscript.

Additional information

Supplementary information accompanies this paper at http://www.nature.com/scientificreports

Competing financial interests: The authors declare no competing financial interests.

How to cite this article: Ai, W. *et al.* A Novel Graphene-Polysulfide Anode Material for High-Performance Lithium-Ion Batteries. *Sci. Rep.* **3**, 2341; DOI:10.1038/srep02341 (2013).